

Conductivity Switching and Electronic Memory Effect in Polymers with Pendant Azobenzene Chromophores

Siew Lay Lim,^{†,‡} Na-Jun Li,[§] Jian-Mei Lu,[§] Qi-Dan Ling,[‡] Chun Xiang Zhu,^{||} En-Tang Kang,^{*,‡} and Koon Gee Neoh[‡]

NUS Graduate School of Integrative Sciences and Engineering (NGS), Department of Chemical and Biomolecular Engineering, and SNDL, Department of Electrical and Computer Engineering, National University of Singapore, 10 Kent Ridge, Singapore 119260, Singapore, Key Laboratory of Organic Synthesis of Jiangsu Province, College of Chemistry and Chemical Engineering, Suzhou University, Suzhou, Jiangsu 215006, People's Republic of China

ABSTRACT Electronic memory devices having the indium–tin oxide/polymer/Al sandwich structure were fabricated from polymers containing pendant azobenzene chromophores in donor–acceptor structures. The reversibility, or rewritability, of the high-conductivity (ON) state was found to be dependant on the terminal moiety of the azobenzene chromophore. While the polymers with electron-accepting terminal moieties (–Br or –NO₂) in the pendant azobenzene exhibit write-once, read-many-times (WORM) type memory behavior, those with electron-donating terminal moieties (–OCH₃) exhibit rewritable (FLASH) memory behavior. The WORM memory devices have low switching (“write”) voltages below –2 V and high ON/OFF current ratios of about 10⁴–10⁶. The polarity of the “write” voltage can be reversed by using an electrode with a higher work function than Al, thus excluding metallic filamentary conduction as a cause of the bistable switching phenomenon. The FLASH memory devices have low “write” and “erase” voltages of about –1.7 to –1.8 V and 2.0 to 2.2 V, respectively, and ON/OFF current ratios of about 10³–10⁴. The electrical bistability observed can be attributed to charge trapping at the azobenzene chromophores, resulting in the charge-separated, high-conductivity state. The proposed mechanism is supported experimentally by a red shift and peak broadening in the UV–visible absorption spectra of the polymer films resulting from the OFF-to-ON electrical transition.

KEYWORDS: azobenzene • charge trapping • electron acceptor • electron donor • conductance switching • polymer memory

1. INTRODUCTION

Organic materials exhibiting electrically bistable behavior (1) are being extensively investigated as an alternative for future data storage applications. A wide range of materials, including conjugated molecules and polymers (2–4) and dopant (5) and complex systems (6, 7), have been utilized in the fabrication of different types of memories, such as write-once, read-many-times (WORM) memory, rewritable or FLASH memory, and dynamic random access memory. The electronic memory behavior was highly dependent on the chemical structure of the materials, which dictated properties such as the occurrence of charge transfer (8–10), conformation change (11–13), and charge trapping (14–16), among others. Azobenzene polymers, owing to their potential applications in optical data storage, nonlinear optics, holographic memories, waveguide switches, and other photonic devices, have received considerable

attention in recent years (17, 18). Photoinduced anisotropy in azobenzene polymers, due to trans–cis isomerization and the orientation effects of the azobenzene chromophore, has been utilized in the formation of surface relief grating for holographic optical storage (19). In particular, the high photosensitivity of the azo dye molecules makes azobenzene polymers popular for use as optical and electronic materials. Photoaddressable polymers with azobenzene chromophores and mesogenic side groups are promising recording materials for optical data storage applications, such as high-capacity DVDs (“digital versatile disc” or “digital video disc”) and holographic memory (20).

Besides optical manipulation, the conformation of azobenzene molecules can also be controlled by electronic means. Recently, experimental evidence indicates that the isomerization of azobenzene (21) and azobenzene derivatives, Disperse Orange 3 (22) and Methyl Orange (23), can be induced by resonant or inelastic tunneling of electrons or by an electric field (24). A sharp increase in the tunneling current is observed when isomerization occurs. The conformation change of a photoactive isomer through an electronic process at the single-molecule level, with an associated rectification effect, has also been reported (25). These reports have demonstrated the potential of azobenzene molecules to function as molecular switches at the nanoscale.

In addition to molecular switches, electronic memories based on voltage-induced electrical bistability in polymers

* To whom all correspondence should be addressed. Tel: +65-6874-2189. Fax: +65-6779-1936. E-mail: cheket@nus.edu.sg.

Received for review August 14, 2008 and accepted October 10, 2008

[†] NUS Graduate School of Integrative Sciences and Engineering (NGS), National University of Singapore.

[‡] Department of Chemical and Biomolecular Engineering, National University of Singapore.

[§] Suzhou University.

^{||} SNDL, Department of Electrical and Computer Engineering, National University of Singapore.

DOI: 10.1021/am800001e

© 2009 American Chemical Society

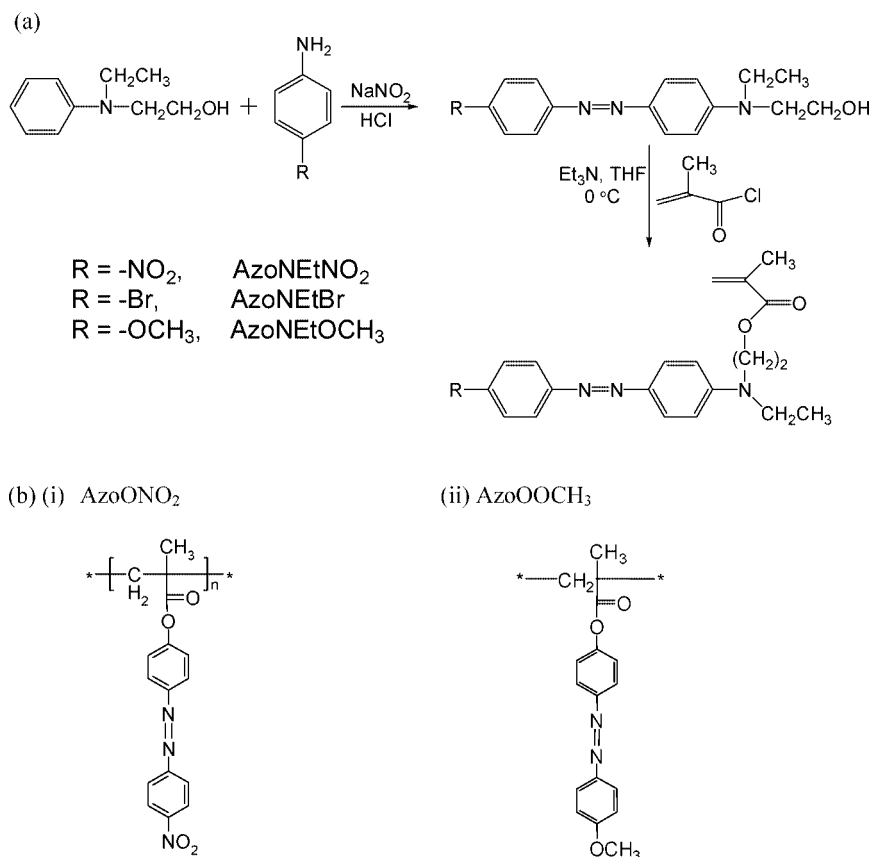


FIGURE 1. (a) Synthesis scheme and molecular structures of the amino-group-containing azobenzene polymers: AzoNEtNO₂, AzoNEtOCH₃, and AzoNEtBr. (b) Molecular structures of the ester-oxygen-containing azobenzene polymers: AzoONO₂ and AzoOOCH₃.

with an azobenzene group in the main chain have also been reported (26). The conduction mechanism is attributed to a voltage-induced trans-to-cis isomerization. In this work, we report the voltage-induced conductance switching behavior and associated memory effects of polymers with pendant azobenzene chromophores in different donor–acceptor structures. The molecular structures of the five azobenzene polymers, AzoNEtNO₂ (>N–Azo–NO₂), AzoNEtOCH₃ (>N–Azo–OCH₃), AzoNEtBr (>N–Azo–Br), AzoONO₂ (–O–Azo–NO₂), and AzoOOCH₃ (–O–Azo–OCH₃), are shown in Figure 1. On the basis of the electrical switching of these materials, an operating mechanism based on charge trapping at the pendant azobenzene chromophore is proposed. The reversibility of charge trapping, and thus the volatility of the memory effect, is determined by the strength of the donors and acceptors. The WORM memory effect is observed in memory devices based on pendant azobenzene chromophores containing nitro and bromo (acceptor) terminal moieties, while the FLASH-type memory effect is observed in those based on pendant chromophores containing methoxy (donor) terminal moieties. The difference in the other substituents linking the azobenzene chromophore to the polymer backbone (amino nitrogen and ester oxygen) does not appear to have an effect on the type of memory behavior observed.

2. EXPERIMENTAL SECTION

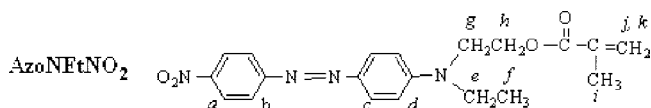
2.1. Materials. 4-Nitroaniline, 4-methoxyaniline, triethylamine, and 2,2'-azobis(isobutyronitrile) (AIBN) were all pur-

chased from Shanghai Chemical Reagent Co. Ltd. as analytical reagents and used as received. Methacryloyl chloride was obtained from Haimen Best Fine Chemical Industry Co. Ltd. and used after distillation. *N*-Ethyl-*N*-(2-hydroxyethyl)aniline was purchased from Tokyo Kasei Kogyo Co. Ltd. and used as received. Tetrahydrofuran (THF) and *N,N*-dimethylformamide (DMF) were purified by vacuum distillation. Other solvents and reagents, such as methanol, acetone, isopropyl alcohol, and *N,N*-dimethylacetamide (DMAc), were obtained from Fisher Scientific (part of Thermo Fisher Scientific Inc.) and used as received.

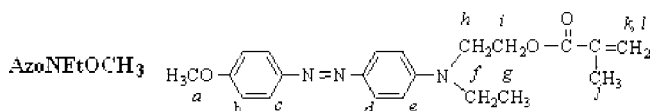
2.2. Materials Characterization. ¹H NMR spectra of the monomers and polymers in CDCl₃ were obtained on an Inova 400 MHz FT-NMR spectrometer at ambient temperature. Molecular weights (*M_n*) and polydispersity (*M_w*/*M_n*) were measured by gel permeation chromatography (GPC) utilizing a Waters 515 pump and a differential refractometer. THF was used as a mobile phase at a flow rate of 1.0 mL/min. The Fourier transform infrared (FTIR) spectra of the organic intermediates and polymers were recorded on a Perkin-Elmer 577 FTIR spectrophotometer, with the samples dispersed in KBr disks. UV–visible absorption spectra were measured on a Shimadzu UV-1601 UV–visible spectrophotometer.

2.3. Preparation of AzoNEtNO₂, AzoNEtOCH₃, and AzoNEtBr. The respective monomers for the three polymers were prepared as detailed in Figure 1a. AzoNEtNO₂ was prepared in three steps: (1) synthesis of the azobenzene intermediate, 2-{ethyl-[4-(4-nitrophenylazo)phenyl]amino}ethanol, from the reaction of 4-nitrobenzenamine with 2-(*N*-ethyl-*N*-phenylamino)ethanol in the presence of hydrochloric acid and deionized water in an ice bath, (2) synthesis of the monomer from the reaction of the azobenzene intermediate with methacryloyl chloride in the presence of triethylamine and dry THF, (3) polymerization of monomer via free-radical polymerization in the presence of AIBN (0.5 mol %) initiator. The polymerization

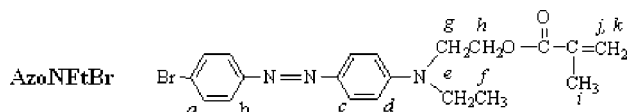
was carried out at 70 °C in DMF and under a nitrogen atmosphere for 4 days. The polymerization mixture was diluted with 5 mL of THF, and the polymer was precipitated in 100 mL of methanol under vigorous stirring. The resulting solid was further washed with excess methanol and finally dried in a vacuum oven at 50 °C for 24 h. The AzoNEtOCH₃ and AzoNEtBr homopolymers were prepared under similar polymerization conditions. The chemical structures of all of the monomers were determined by ¹H NMR spectroscopy.



¹H NMR (CDCl₃): δ (ppm) 8.31 (2H, *a*), 7.94–7.90 (4H, *b* and *c*), 6.81 (2H, *d*), 6.11 (1H, *k*), 5.59 (1H, *j*), 4.39 (2H, *h*), 3.72 (2H, *g*), 3.53 (2H, *e*), 1.94 (3H, *i*), 1.27 (3H, *f*). Elem anal. Calcd for C₂₀H₂₂N₄O₄: C, 62.83; H, 5.76; N, 14.66. Found: C, 62.64; H, 5.94; N, 14.51.

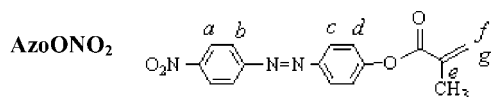


¹H NMR (CDCl₃): δ (ppm) 7.83–7.81 (4H, *c* and *d*), 6.98 (2H, *b*), 6.80 (2H, *e*), 6.09 (1H, *k*), 5.57 (1H, *l*), 4.34 (2H, *i*), 3.70 (3H, *a*), 3.66 (2H, *h*), 3.48 (2H, *f*), 1.93 (2H, *j*), 1.23 (3H, *g*). Elem anal. Calcd for C₂₁H₂₅N₃O₅: C, 60.72; H, 6.02; N, 10.12. Found: C, 60.21; H, 6.52; N, 10.34.

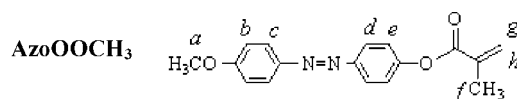


¹H NMR (CDCl₃): δ (ppm) 7.88 (2H, *b*), 7.73 (2H, *c*), 7.60 (2H, *a*), 6.82 (2H, *d*), 6.11 (1H, *k*), 5.58 (1H, *j*), 4.38 (2H, *h*), 3.71 (2H, *g*), 3.50 (2H, *e*), 1.94 (3H, *i*), 1.25 (3H, *f*). Elem anal. Calcd for C₂₀H₂₂N₃BrO₂: C, 57.69; H, 5.29; N, 10.10. Found: C, 57.59; H, 5.48; N, 9.89.

2.4. Preparation of AzoONO₂ and AzoOOCH₃. AzoONO₂ and AzoOOCH₃ were synthesized and characterized as reported in the literature (27).



¹H NMR (CDCl₃): δ (ppm) 8.37 (2H, *a*), 8.09 (4H, *b* and *c*), 7.07 (2H, *d*), 2.09 (3H, *e*), 6.17 (1H, *f*), 5.62 (1H, *g*). Elem anal. Calcd for C₁₆H₁₃N₃O₄: C, 61.74; H, 4.18; N, 13.50. Found: C, 61.83; H, 4.19; N, 13.50.



¹H NMR (CDCl₃): δ (ppm) 3.89 (3H, *a*), 7.01 (2H, *b*), 7.93 (4H, *c* and *d*), 7.29 (2H, *e*), 2.08 (3H, *f*), 6.39 (1H, *g*), 5.80 (1H, *h*). Elem anal. Calcd for C₁₇H₁₆N₂O₅: C, 68.92; H, 5.41; N, 9.46. Found: C, 68.94; H, 5.44; N, 9.41.

The chemical structures of all of the polymers were identified by FTIR and ¹H NMR. The IR spectra confirmed the chemical structures, which exhibited all absorption bands attributed to

Table 1. Number-Average Molecular Weight (*M_n*), Polydispersity (*M_w/M_n*), and Glass Transition Temperature (*T_g*) of the Azobenzene Polymers

polymer	GPC result		glass transition temperature, <i>T_g</i> (°C)
	<i>M_n</i>	<i>M_w/M_n</i>	
AzoONO ₂	2780	1.25	118
AzoOOCH ₃	3400	1.36	121
AzoNEtNO ₂	4030	1.89	145
AzoNEtBr	5700	1.67	120
AzoNEtOCH ₃	5150	1.56	112

functional groups present in the polymers. The IR spectrum of each polymer is similar to its monomer, except for the substantial weakening of the absorption bands at 3080 and 1608 cm⁻¹, attributed to the C=C bonds, due to vinyl polymerization.

2.5. Fabrication and Measurement of the Memory Devices. The indium–tin oxide (ITO) glass substrate was pre-cleaned with water, acetone, and isopropyl alcohol, in that order, in an ultrasonic bath for 20 min. The DMAC solution of the azobenzene polymer (10 mg/mL) was spin-coated onto ITO, and the solvent was removed in a vacuum chamber at 10⁻⁵ Torr and 60 °C for 10 h. The thickness of the polymer film was about 50 nm, as determined from the edge profile of the atomic force microscopy image. Al top electrodes of about 300 nm in thickness were thermally evaporated and deposited onto the polymer surface at about 10⁻⁷ Torr through a shadow mask. Active device areas of 0.0016, 0.0004, and 0.000 225 cm² were obtained. All electrical properties of the device were characterized under ambient conditions, without any encapsulation, using a Hewlett-Packard 4156A semiconductor parameter analyzer equipped with an Agilent 16440A SMU/pulse generator. Electrical measurements with a liquid-Hg electrode were performed by placing a Hg droplet on the polymer film spin-coated on ITO. A voltage sweep was applied using the Keithley 238 High Current Source Measurement Unit, with the probe contacts on ITO or Hg.

3. RESULTS AND DISCUSSION

3.1. Material Properties. The AzoNEtNO₂ polymer has a weight-average molecular weight of about 4030 and a polydispersity index of about 1.89, as revealed by GPC measurement. The polymer exhibited good thermal stability, with an onset decomposition temperature of about 250 °C and a glass transition temperature (*T_g*) of about 145 °C, as determined by thermogravimetric analysis and differential scanning calorimetry, respectively. The corresponding properties of the remaining four polymers, namely, AzoNEtOCH₃, AzoNEtBr, AzoONO₂, and AzoOOCH₃, are summarized in Table 1. The thermal decomposition temperatures of all of the polymers are around 250 °C.

The UV–visible absorption spectra of the azobenzene polymers in dilute DMAC solutions are shown in Figure 2a. All of the spectra exhibit two major absorption peaks. The absorption peak at the shorter wavelength is attributed to the π–π* electronic transition of the aromatic ring, while the peak at the longer wavelength is due to charge transfer (CT) in the azobenzene chromophore. The difference in the relative intensities of the two absorption peaks and in the position of the CT absorption peaks of the azobenzene polymers can be attributed to the difference in the degree of CT interaction, and thus electron delocalization, in the azobenzene chromophores.

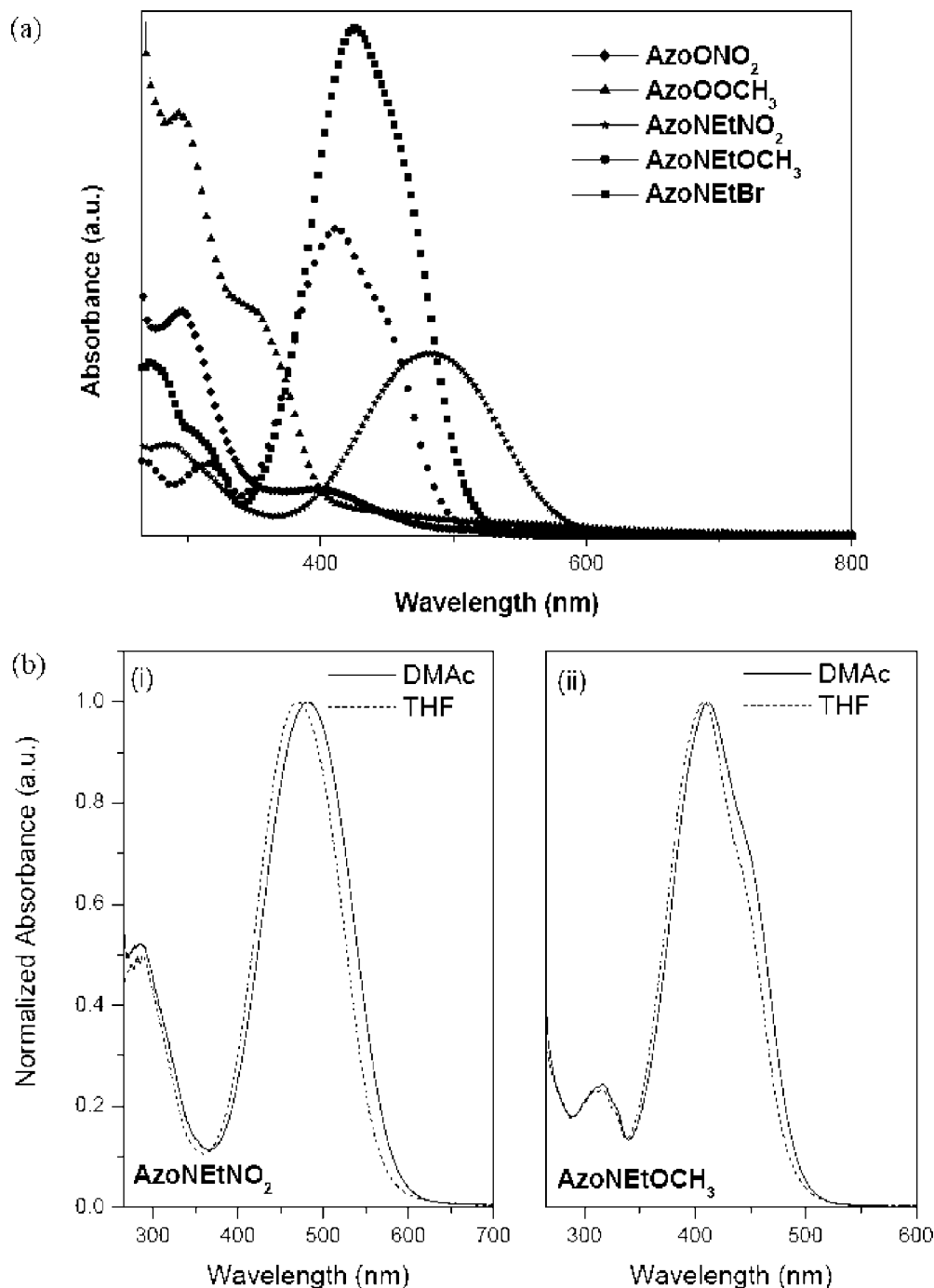


FIGURE 2. UV–visible absorption spectra of (a) the five azopolymers in a dilute DMAC solution and of (b) (i) AzoNEtNO₂ and (ii) AzoNEtOCH₃ in dilute DMAC and THF solutions, respectively.

The UV–visible spectrum of AzoNEtNO₂ exhibits two bands centered at around 285 and 483 nm. The former is attributed to the π – π^* electronic transition of the aromatic ring and the latter, with higher intensity, to the vibronic coupling between n – π^* and π – π^* electronic transitions of the *trans*-azobenzene chromophore (28). The latter absorption is due to the high degree of CT interaction between the electron donor (amino group) and the electron acceptor (nitro group). The UV–visible absorption spectrum of AzoONO₂ in a dilute DMAC solution exhibits two bands centered at around 295 nm (π – π^* electronic transition of the aromatic ring) and 396 nm (CT of the azobenzene

chromophore). The CT absorption band of the azobenzene chromophore of AzoONO₂ appears at a shorter wavelength, compared to that of AzoNEtNO₂. Because of the weaker electron-donating characteristic of the ester oxygen, as compared to that of the amino nitrogen, π -electron delocalization in the conjugated system of AzoONO₂ is reduced, resulting in an increase in the energy of the π – π^* transition. The spectra of the other polymers can be interpreted in a similar manner.

The polymers with different terminal electron donor and acceptor groups in the azobenzene side chains exhibit a significant positive solvatochromic shift for the lowest en-

ergy π - π^* transition. Figure 2b shows the UV-visible absorption spectra of AzoNEtNO₂ and AzoNEtOCH₃ in THF and DMAc. The respective solvents have dielectric constants of 7.6 and 37.8. The wavelength of the lower energy absorption peak of AzoNEtNO₂ shows a shift from 469 nm in THF to 483 nm in DMAc, while that of AzoNEtOCH₃ shows a corresponding shift from 408 to 418 nm. This shift is associated with the fact that, upon an increase in the solvent polarity, the dipolar character of the excited state is increased (i.e., the ground state is characterized by the formula DA, while D⁺A⁻ characterizes the excited state) (29). A large positive difference in the dipole moment between the electronic ground state and the CT excited state is thus produced. The dipole moment of 4-methoxy-4'-nitroazobenzene, a suitable model compound for the azobenzene chromophore in AzoONO₂, is 5.63 D in the ground state and 8.15 D in the excited state (30). Thus, a red shift in the absorption wavelength can serve as an indication of an overall increase in the dipole moment or polarity of the local environment (solvent in a solution or the polymer matrix in a thin film).

Experimental values of the highest occupied molecular orbital (HOMO), lowest unoccupied molecular orbital (LUMO), and band gap of each of the polymers were obtained by cyclic voltammetry and UV-visible spectroscopy (31, 32). During the anodic scan, AzoNEtNO₂ exhibits irreversible p-doping behavior, with an oxidation peak at about 1.1 V vs Ag/AgCl. The peak can be attributed to the irreversible oxidation of the azobenzene chromophore. The results suggest that the azobenzene chromophore tends to donate electrons and is an efficient hole-transport site. The HOMO energy level can be calculated from the onset oxidation potential [$E_{\text{Ox}}(\text{onset})$] based on the reference energy level of ferrocene (4.8 eV below the vacuum level, which is defined as zero)

$$\text{HOMO} = -[E_{\text{Ox}}(\text{onset}) - E_{\text{Foc}} + 4.8] \text{ eV}$$

$$\text{LUMO} = \text{HOMO} + E_g(\text{band gap})$$

wherein E_{Foc} is the potential of the external standard, the ferrocene/ferricenium ion (Foc/Foc⁺) couple. The value of E_{Foc} , determined under the same experimental conditions, is about 0.38 eV vs Ag/AgCl. $E_{\text{Ox}}(\text{onset})$ for AzoNEtNO₂ is about +1.00 eV vs Ag/AgCl, giving a HOMO energy level of about -5.43 eV relative to the vacuum level. The energy band gap corresponding to the HOMO \rightarrow LUMO transition of AzoNEtNO₂ was obtained as about 2.14 eV from the absorption edge of the UV-visible absorption spectrum, giving a corresponding LUMO energy level of about -3.30 eV. The HOMO energy levels, energy band gaps, and corresponding LUMO energy levels of all of the polymers studied are summarized in Table 2.

3.2. Electrical Characterization. Memory devices of an ITO/polymer/Al sandwich structure were fabricated using thin films of the five azobenzene polymers. The device structure is shown schematically in Figure 3a.

Electrical transitions in the ITO/polymer/Al devices were observed in the measurements of the current response to an external applied voltage. ITO was maintained as the ground electrode in all electrical measurements. The current

Table 2. HOMO and LUMO Energy Levels Obtained from Cyclic Voltammetry and UV-Visible Spectroscopy

polymer	HOMO (eV)	LUMO (eV)	E_g (eV)
AzoONO ₂	5.53	2.99	2.54
AzoOOCH ₃	5.80	2.72	3.08
AzoNEtNO ₂	5.43	3.29	2.14
AzoNEtBr	5.43	2.98	2.45
AzoNEtOCH ₃	5.33	2.82	2.51

density-voltage (J - V) characteristics of the ITO/AzoNEtNO₂/Al device in Figure 3b show two distinct conductivity states. The device is initially in the low-conductivity (OFF) state, with a current density of about 10^{-6} A/cm² at -1 V when a voltage sweep was applied starting from 0 V. When the voltage applied was increased further, the device switches from the OFF state to the high-conductivity (ON) state at a threshold voltage of about -1.5 V, as indicated by the abrupt increase of the current density to about 10^{-1} A/cm² (sweep 1). The high current density observed during the subsequent voltage sweep indicates retention of the ON state in the device (sweep 2). The ON-state J - V curves under negative and opposite biases were symmetrical. The transition from the OFF state to the ON state serves as the "write" process for the memory device. The ON state of the device could be distinguished from the OFF state by an ON/OFF current ratio of about 10^4 when read at -1 V. The AzoONO₂ polymer, having the same nitro group as the acceptor moiety but with an ester oxygen as the donor moiety, also exhibits similar behavior in a device. The ITO/AzoONO₂/Al device undergoes an OFF-to-ON transition at about -1.8 V and remains in the ON state during the following voltage sweep (Figure 3d). The ratio of the ON- and OFF-state currents is about 10^6 when the device is read at -1 V. After undergoing the OFF-to-ON transition, both devices remain in their ON states even after the electrical power has been turned off and cannot be returned to the low-conductivity state by applying a reverse bias. This behavior is characteristic of a WORM memory device. The ON and OFF states of the devices are stable for up to 10^8 continuous read pulses of -1 V (pulse period = 2 μ s, pulse width = 1 μ s) without any resistance degradation. The high ON/OFF current ratios of the devices promise a low misreading rate by precise control over the OFF and ON states. The retention ability of the OFF and ON states of a device is tested by first subjecting a device in the OFF state to a constant voltage stress of -1 V and recording the current passing through the device at regular intervals. The device is then programmed by a voltage sweep, and the ON state is evaluated under the same stress conditions. Parts c and e of Figure 3 and show that each device has both stable OFF- and ON-state currents within the 3 h time frame, with the high ON/OFF current ratio sustained.

When the nitro terminal moiety in the azobenzene side chain of the polymer was replaced by the methoxy group, different electrical behavior was observed. For the ITO/AzoOOCH₃/Al device, an abrupt increase in the current density was observed at about -1.8 V when a voltage sweep from 0 to -3 V was applied (sweep 1) (Figure 4a). The high-

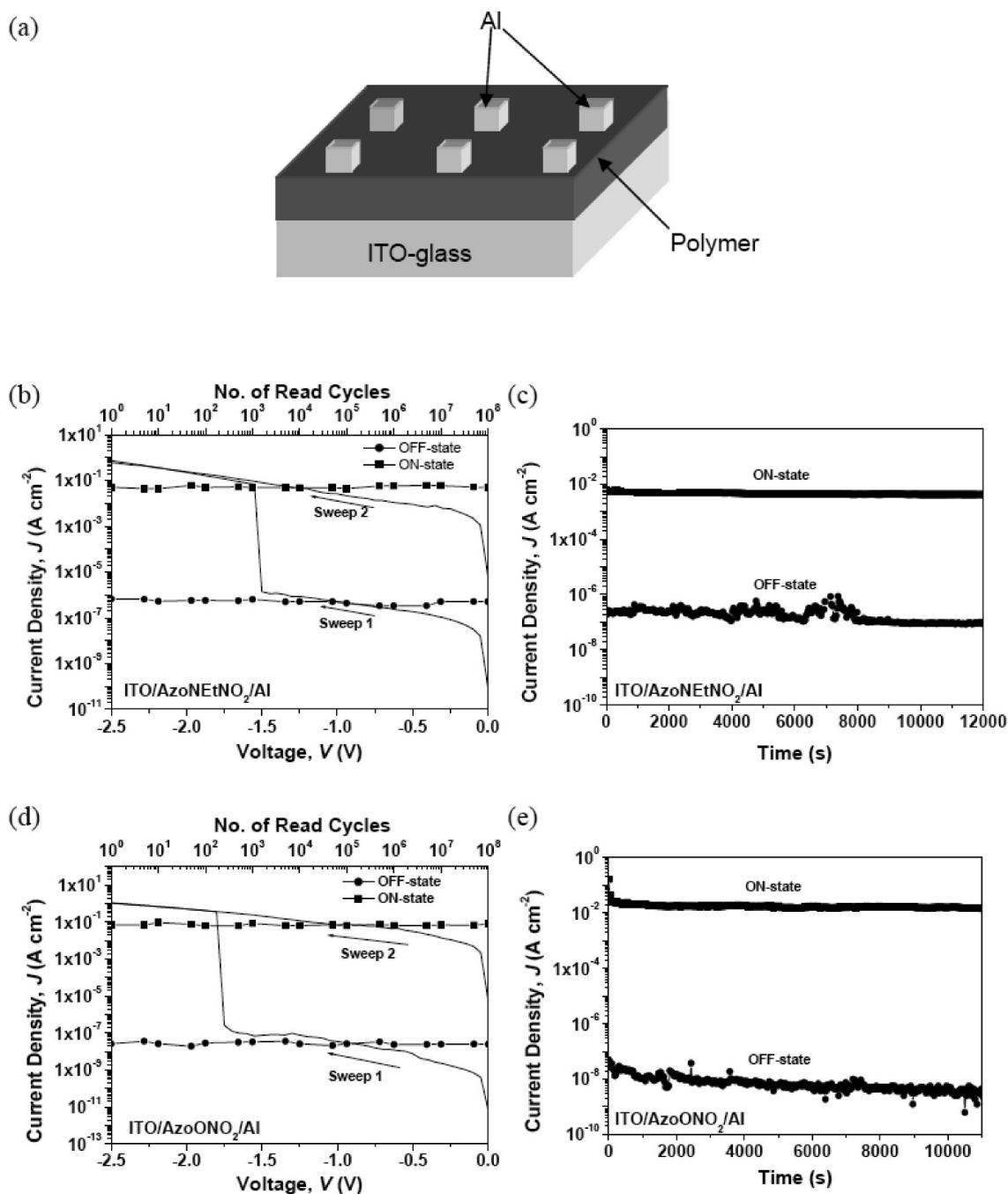


FIGURE 3. (a) Schematic diagram of the polymer memory device consisting of a thin film of the azobenzene polymer sandwiched between an ITO bottom electrode and an Al top electrode. Current density–voltage (J – V) characteristics and effect of the operation time (at -1 V) on the device current density in the OFF and ON states of the ITO/AzoNEtNO₂/Al device (b and c) and the ITO/AzoONO₂/Al device (d and e).

conductivity ON state was retained when the voltage sweep was applied again (sweep 2). In a voltage sweep of opposite bias from 0 to 3 V (sweep 3), an abrupt decrease in the current density was observed at a threshold voltage of about 2.2 V, indicating a device transition from the ON state back to the OFF state. This electrical transition represents the “erase” process for the memory device. The device remains in the OFF state during the following positive sweep (sweep 4). The “erased” state can be further converted to the “written” state when the switching threshold voltage of about -1.8 V was reapplied, indicating that the memory device was rewritable (sweep 5). Both the low- and high-

conductivity (OFF and ON) states of the device were stable under power-off conditions and under constant voltage stress conditions of -1 V, allowing an ON/OFF current ratio of about 10^4 to be maintained when read at -1 V (Figure 4b). The ability of the device to undergo write, read, and erase cycles fulfills the functionality of a FLASH memory device. The ITO/AzoNEtOCH₃/Al device showed a similar reversible switching behavior, with “write” and “erase” voltages of -1.7 and 2.0 V, respectively, and an ON/OFF current ratio of about 10^3 at -1 V (Figure 4c). The stability of the two bistable states under constant voltage stress was similarly evaluated at -1 V (Figure 4d).

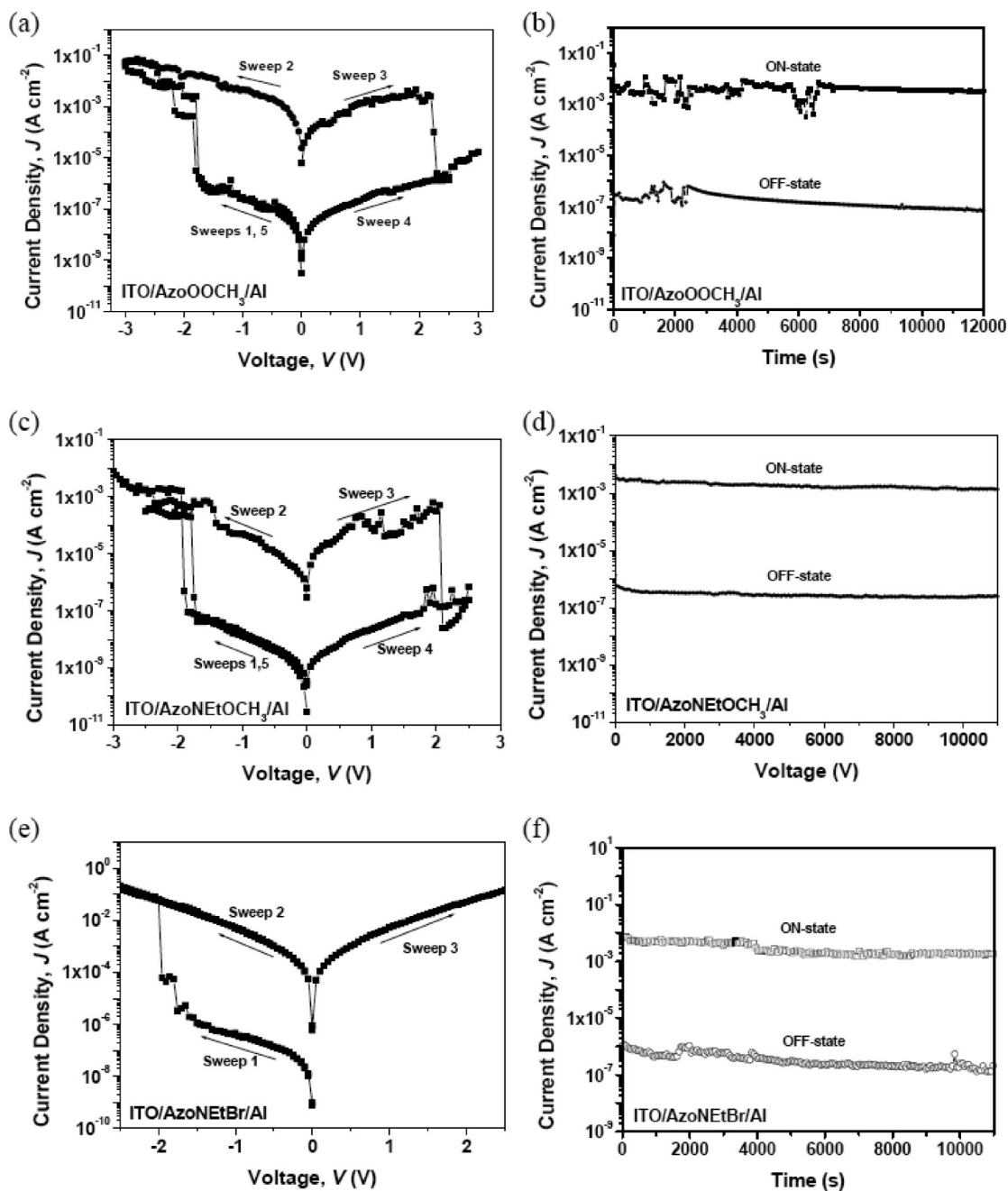
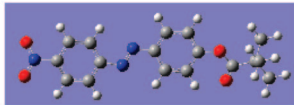
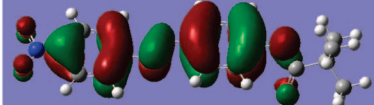
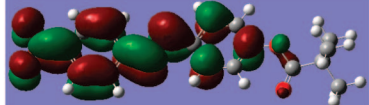
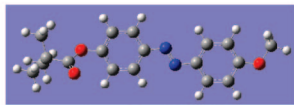
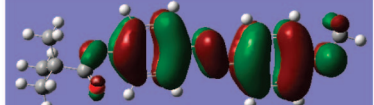
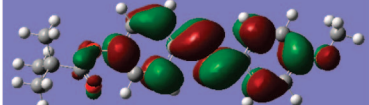
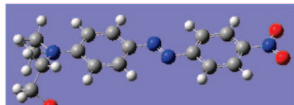



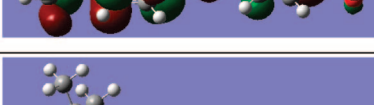
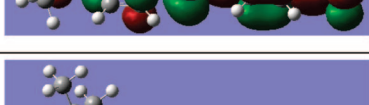
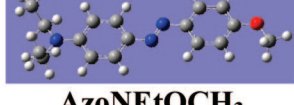
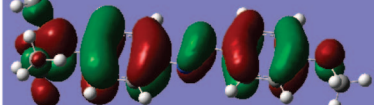
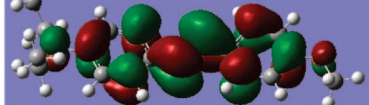


FIGURE 4. Current density–voltage (J – V) characteristics and the effect of the operation time (at -1 V) on the device current density in the OFF and ON states of the ITO/AzoOOCH₃/Al rewritable device (a and b), the ITO/AzoNEtOCH₃/Al rewritable device (c and d), and the ITO/AzoNEtBr/Al WORM device (e and f).

Considering the differences between the nitro and methoxy groups, with the former possessing electron-accepting characteristics and the latter electron-donating characteristics, the reversibility of the “written” state, or the ON state, must be dependent on the donor/acceptor nature of the terminal moiety of the azobenzene chromophore. Thus, the electrical switching behavior of another azobenzene polymer with a bromo terminal moiety, AzoNEtBr, in a memory device was also investigated. The bromo group also possesses the electron-accepting property but is a weaker acceptor in comparison with the nitro moiety. As shown by the J – V characteristics of the ITO/AzoNEtBr/Al device, the behavior of the memory device is of the WORM type, with

a switching threshold voltage of -1.9 V and an ON/OFF current ratio of about 10^4 (Figure 4e). The stability of the two conductivity states of the WORM device is demonstrated by the almost constant current densities observed when the device was placed under constant voltage stress for a period exceeding 3 h (Figure 4f). From the electrical characteristics of AzoNEtNO₂, AzoONO₂, and AzoNEtBr, it can be seen that the transition of the device from the OFF state to the ON state is irreversible when the terminal moiety of the azobenzene chromophore is electron-accepting in nature and is reversible when the terminal moiety is electron-donating. Thus, charge trapping, mediated by the terminal moieties of the pendant azobenzene chromophores, is probably

Table 3. HOMO and LUMO Surfaces of the Monomer Units of the Azobenzene Polymers Obtained by Simulation

Basic Unit of Polymer	HOMO	LUMO
 AzoONO₂		
 AzoOOCH₃		
 AzoNEtNO₂		
 AzoNEtOCH₃		
 AzoNEtBr		

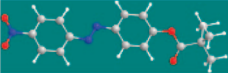
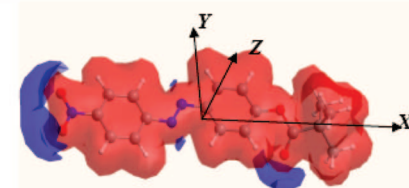
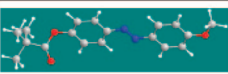
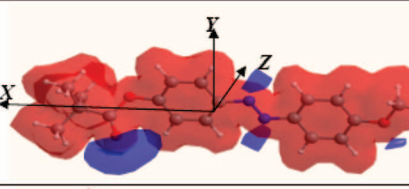
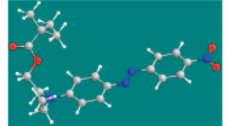
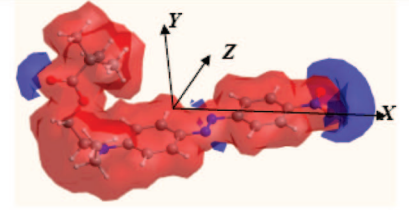
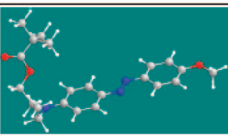
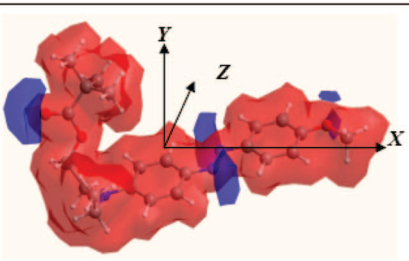
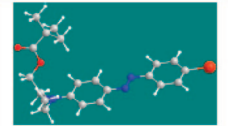
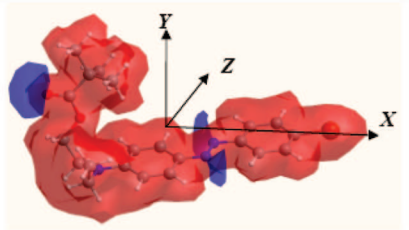
responsible for the conductance switching and the associated memory behavior.

In previous works, rewritable and non-rewritable resistive switching memories have been fabricated, respectively, from functional polyimide polymers containing electron-donating and -accepting moieties in the main chain and an acrylate polymer with electroactive carbazole pendant groups (9, 11). On the basis of the unique properties and characteristics of the polymers and their structures, a mechanism of CT between the donors and acceptors is proposed for the field-induced conductivity changes in the rewritable polymer memory, while a mechanism of conformation change of the pendant groups is proposed for the non-rewritable polymer memory. Azobenzene compounds, such as Sudan I and Disperse Red I, are capable of trapping and storing an electrical charge for long periods of time and are promising for electrooptical information storage (33). Because the polymers studied in this work contain similar azobenzene chromophores in the side chains, the ability of the azoben-

zene chromophores to trap and store charges is likely to play an important role in the electrical bistability observed.

Molecular simulation of the monomer units of the azobenzene polymers was carried out at the density functional theory B3LYP/6-31G(d) level with the *Gaussian 03* program package (34) to obtain physical properties such as molecular orbitals and electrostatic potentials (ESPs). The HOMO and LUMO surfaces for the five polymers are shown in Table 3. The HOMO and LUMO surfaces obtained are generally asymmetric, with the former more localized on the electron-donor side and the latter on the electron-acceptor side. Such localization of the electron density in the HOMOs results in large ground-state dipole moments. Upon HOMO \rightarrow LUMO excitation, a larger dipole moment is formed for the excited state because of the considerable increase in charge separation. The feasibility of forming a charge-separated state in a compound can therefore be inferred from the locations of the HOMO and LUMO, as well as the change in the electron density distribution upon excitation.

Table 4. Molecular ESP Surfaces and Quadrupole Moments (Field-Independent Basis, Debye–Ång) of the Monomer Units Obtained from Simulation

Basic Unit of Polymer	Electrostatic Potential (ESP) surface and quadrupole moment (field-independent basis, Debye–Ång)
 AzoONO₂	 XX : -170.1 YY : -131.4 ZZ : -139.7
 AzoOOCH₃	 XX : -91.1 YY : -127.3 ZZ : -138.2
 AzoNEtNO₂	 XX : -241.1 YY : -156.7 ZZ : -164.4
 AzoNEtOCH₃	 XX : -189.9 YY : -159.6 ZZ : -167.4
 AzoNEtBr	 XX : -150.5 YY : -155.5 ZZ : -161.8

The molecular ESP surfaces show the presence of some negative regions that are associated with the electron-acceptor groups (Table 4). The negative regions can serve as “traps” to block the mobility of the charge carriers. In the OFF state, the device current is low because injected holes are trapped by the negative ESP regions while hopping along the pendant azobenzene chromophores. At the switching voltage, the majority of the traps are filled and a “trap-free” environment with higher charge mobility is formed. The device is therefore transformed into the high-conductivity ON state. Rewritable memory behavior is observed when the trapped charges can be detrapped by applying a reverse bias, while WORM memory behavior is observed when detrapping does not occur under a nondegrading reverse bias.

Azobenzenes with donor–acceptor structures, such as those found in the azobenzene polymers in this work, have large permanent dipole moments that favor holding of the trapped charges (33). An internal electric field is created, thus maintaining the high-conductivity state. The polar characters of the azobenzene chromophores in the azopolymers can be determined by the quadrupole moments of the monomer units obtained from simulation (Table 4). The large quadrupole moments of the monomer units are consistent with the localization of the electron density in the HOMOs. Azobenzene chromophores with donor–acceptor structures also have significant potential for intramolecular CT through the presence of donor and acceptor groups in a conjugated structure (35). When the terminal moieties of the azobenzene chromophore are electron acceptors, trapped charges

are stabilized by intramolecular CT to form a charge-separated state. The filled traps may not be easily detrapped under nondegrading reverse fields, resulting in a high-conductivity state that can be retained for a long time in the nitro- and bromo-containing azobenzene polymers (AzoONO₂, AzoNEtNO₂, and AzoNEtBr). WORM memory behavior is thus observed in these devices. Azobenzene chromophores that contain electron donors as terminal moieties are not able to undergo intramolecular CT to form charge-separated states. The trapped charges can therefore be detrapped by reverse bias, as observed in the rewritable memory properties of the methoxy-containing azobenzene polymers (AzoOOCH₃ and AzoNEtOCH₃). The electron density transfer between the electron donor and acceptor occurring during the intramolecular CT process in the azobenzene chromophore under an electric field is akin to the HOMO → LUMO transition induced by photoexcitation (36) because the HOMO and LUMO are localized over the electron donor and acceptor, respectively. The significant overlap of the two orbitals in the mid-region of the π -conjugated system facilitates such an electron density transfer. An analysis of the HOMO and LUMO surfaces of AzoONO₂ shows that, upon undergoing the HOMO → LUMO transition, the electron density shifts from the donor side and becomes more localized on the acceptor side, forming a charge-separated state. However, when the electron-accepting -NO₂ moiety of the azobenzene chromophore is substituted by the electron-donating -OCH₃ moiety in AzoOOCH₃, the change in the electron density from the HOMO → LUMO transition is less significant. The formation of a charge-separated state in AzoONO₂ and the lack thereof in AzoOOCH₃, upon undergoing the HOMO → LUMO transition, are consistent with the different memory behavior observed.

The proposed mechanism is supported by the changes observed in the UV–visible absorption spectra of the azobenzene polymer films as a result of the OFF-to-ON state electrical transition. A liquid-Hg droplet was used as the top electrode in place of the Al contacts. After application of a voltage sweep across the device, the Hg electrode was removed and the resultant polymer film analyzed by UV–visible absorption spectroscopy. When the normalized absorption spectra of the azobenzene polymer films in their pristine states (OFF state) are compared to those after a voltage sweep of 0 to -2.5 V has been applied (ON state), a slight red shift and broadening of the CT absorption band of the respective polymer have occurred as a result of the electrical transition (Figure 5). The red shift suggests an increase in the polarity of the local environment due to an increase of the dipole moment of the azobenzene chromophore. The shift is not unlike that observed in the UV–visible absorption spectra of the azobenzene polymers when the solvent polarity is increased. In the solid state, the change can be attributed to an increase in the dipole moment of the azobenzene chromophore as a result of the charge trapping and subsequent intramolecular CT in the polymer film during the OFF-to-ON state electrical transition.

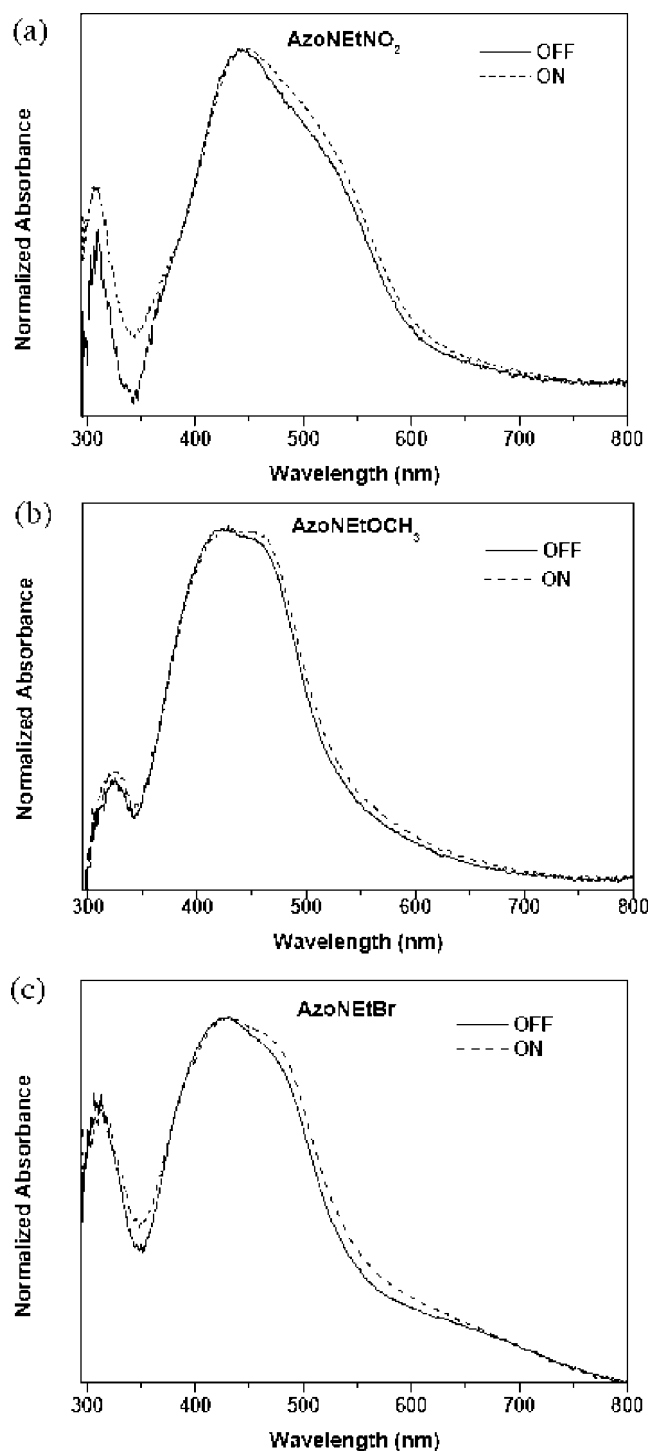


FIGURE 5. Comparison of the UV–visible spectra of the (a) AzoNEtNO₂, (b) AzoNEtBr and (c) AzoNEtOCH₃ polymer thin films in the low-conductivity (OFF) and high-conductivity (ON) states. The ON state was induced using a removable liquid-Hg droplet as the top electrode.

The formation of conduction filaments under high electric fields has resulted in electrical transitions in some polymer films (37, 38). In all of the azobenzene polymer devices, the current magnitude decreases accordingly when the active device area is reduced (0.0016 → 0.0004 → 0.000225 cm²), giving a current density that is almost constant. Together with the good reproducibility and stability of the memory phenomena observed in the devices, as well as the structure-

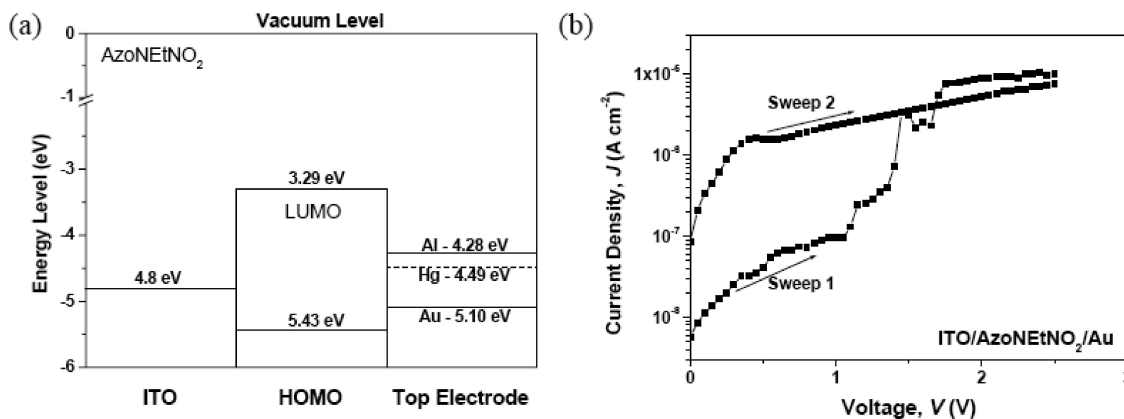


FIGURE 6. (a) Energy level diagram for the ITO/AzoNEtNO₂/metal device with Al, Hg, or Au as the top electrode. (b) Current density–voltage (J – V) characteristics of the ITO/AzoNEtNO₂/Au memory device.

dependent electrical switching behavior, the possibility of electrical transition due to filament conduction and polymer degradation effects can be ruled out. Furthermore, on the basis of an analysis of the barrier heights for charge injection from the electrodes (work function of ITO = 4.8 eV; work function of Al = 4.28 eV) (39, 40), charge injection into the polymer layer via hole injection from ITO to the HOMO of the polymer is more favorable under the applied negative bias. Correspondingly, the WORM devices based on AzoONO₂ and AzoNEtNO₂ exhibit OFF-to-ON transitions only when a negative bias is applied and not when swept positively from 0 to +2.5 V, thus reaffirming that the switching phenomenon observed is intrinsic to the polymeric material. Electrical measurements were also carried out with a cold-deposited liquid-Hg top electrode, instead of the thermally evaporated Al top electrode, with ITO as the ground electrode. The work function of liquid-Hg metal is about 4.5 eV, resulting in a higher energy barrier for electron injection into the LUMO. Because hole injection occurs from the ITO electrode, with hole transport as the main conduction mechanism, the change in the top electrode probably does not have a great effect on the electrical behavior of the devices. Thus, similar conductance switching and the associated memory property were observed in the devices using Hg as the top electrode. The observed memory effect with a different metal electrode provides additional evidence that the memory effect observed is intrinsic to the polymer and not due to external effects associated with the use of an Al electrode (41, 42). The high surface tension of the cold-deposited Hg electrode also reduces the possibility of short circuits if any pinholes were present, as well as damage to the polymer film.

Although the energy barrier for charge injection at the metal/HOMO interface is reduced when the Al top electrode was replaced by Hg, the Hg/HOMO barrier is still larger than the ITO/HOMO barrier (Figure 6a). Hole injection into the HOMO from ITO thus remains more favorable, in comparison with that from the Hg electrode. Hole injection from the metal into the HOMO could be made more favorable by selecting a high work function metal that forms a metal/HOMO interface with an energy barrier smaller than that at the ITO/HOMO interface. Under such circumstances, the

conductance switching is more likely to occur when holes are injected from the metal electrode, i.e., when positive bias is applied with ITO as the ground. This would provide convincing confirmation that the conductance switching observed is intrinsic to the polymer. Also, the “write” voltage could possibly be lowered because of the smaller barrier to charge injection. Accordingly, Au, with a work function of 5.1 eV, is used in place of Al to form the ITO/AzoNEtNO₂/Au device. The J – V characteristics of the device show the OFF-to-ON transition occurring at about 1.1 V during a positive voltage sweep from 0 to 2.5 V and the ON state being retained during the subsequent sweep (Figure 6b). The ON/OFF current ratio of the ITO/AzoNEtNO₂/Au device, about $10^{1.4}$, is lower than that of the ITO/AzoNEtNO₂/Al device. The reduction in the switching voltage by about 0.4 V is comparable to the reduction in the injection barrier height by 0.3 eV when the Al electrode was substituted with Au. Reversals in polarity and reductions in “write” voltages are also observed in similar experiments involving the other azobenzene polymers as the active layer.

4. CONCLUSIONS

Polymers with pendant azobenzene chromophores in donor–acceptor structures have been found to exhibit bistable conductivity switching in ITO/polymer/Al sandwich structures. They are thus potentially useful for application in electronic memory devices. The switching effect was found to be dependent on the donor–acceptor nature of the terminal moiety of the pendant azobenzene chromophore. WORM memory behavior is observed in polymers with terminal acceptor moieties in the pendant structure (AzoONO₂, AzoNEtNO₂, and AzoNEtBr), while rewritable memory behavior is observed in polymers with terminal donor moieties (AzoOOCH₃ and AzoNEtOCH₃). Threshold switching voltages of less than –2 V and high ON/OFF current ratios of 10^4 – 10^6 are observed in the ITO/polymer/Al WORM devices, while “write” and “erase” voltages of –1.7 to –1.8 V and 2.0 to 2.2 V, respectively, and ON/OFF current ratios of 10^3 – 10^4 are observed in the ITO/polymer/Al rewritable memory devices. The electrical bistability observed can be attributed to charge trapping at the azobenzene chromophores. The donor–acceptor electronic struc-

ture of the pendant azobenzene chromophores facilitates intramolecular CT to stabilize the high-conductivity state. The proposed trapping mechanism is supported by observation of a red shift and broadening of the UV-visible absorption spectra of the polymer films after undergoing the OFF-to-ON electrical transition.

REFERENCES AND NOTES

- (1) Stikeman, A. *Technol. Rev.* **2002**, *105*, 31.
- (2) Hong, S. H.; Kim, O.; Choi, S.; Ree, M. *Appl. Phys. Lett.* **2007**, *91*, 093517.
- (3) Wei, D.; Baral, J. K.; Osterbacka, R.; Ivaska, A. *J. Mater. Chem.* **2008**, *18*, 1855–1857.
- (4) Cai, X. Y.; Gerlach, C. P.; Frisbie, C. D. *J. Phys. Chem. C* **2007**, *111*, 452–456.
- (5) Lai, Q. X.; Zhu, Z. H.; Chen, Y.; Patil, S.; Wudl, F. *Appl. Phys. Lett.* **2006**, *88*, 133515.
- (6) Weitz, R. T.; Walter, A.; Engl, R.; Sezi, R.; Dehm, C. *Nano Lett.* **2006**, *6*, 2810–2813.
- (7) Liu, Z. C.; Xue, F. L.; Su, Y.; Varahramyan, K. *IEEE Electron Device Lett.* **2006**, *27*, 151–153.
- (8) Tseng, R. J.; Baker, C. O.; Shedd, B.; Huang, J. X.; Kaner, R. B.; Ouyang, J. Y.; Yang, Y. *Appl. Phys. Lett.* **2007**, *90*, 053101.
- (9) Ling, Q. D.; Chang, F. C.; Song, Y.; Zhu, C. X.; Liaw, D. J.; Chan, D. S. H.; Kwong, D. L.; Kang, E. T.; Neoh, K. G. *J. Am. Chem. Soc.* **2006**, *128*, 8732–8733.
- (10) Mukherjee, B.; Pal, A. J. *Chem. Mater.* **2007**, *19*, 1382–1387.
- (11) Lim, S. L.; Ling, Q. D.; Teo, E. Y. H.; Zhu, C. X.; Chan, D. S. H.; Kang, E. T.; Neoh, K. G. *Chem. Mater.* **2007**, *19*, 5148–5157.
- (12) Xie, L. H.; Ling, Q. D.; Hou, X. Y.; Huang, W. J. *Am. Chem. Soc.* **2008**, *130*, 2120–2121.
- (13) Bandyopadhyay, A.; Miki, K.; Wakayama, Y. *Appl. Phys. Lett.* **2006**, *89*, 243506.
- (14) Kanwal, A.; Chhowalla, M. *Appl. Phys. Lett.* **2006**, *89*, 203103.
- (15) Pearson, C.; Ahn, J. H.; Mabrook, M. F.; Zeze, D. A.; Petty, M. C.; Kamtekar, K. T.; Wang, C. S.; Bryce, M. R.; Dimitrakis, P.; Tsoukalas, D. *Appl. Phys. Lett.* **2007**, *91*, 123506.
- (16) Kondo, T.; Lee, S. M.; Malicki, M.; Domercq, B.; Marder, S. R.; Kippelen, B. *Adv. Funct. Mater.* **2008**, *18*, 1112–1118.
- (17) Lee, M. J.; Jung, D. H.; Han, Y. K. *Mol. Cryst. Liq. Cryst.* **2006**, *444*, 41–50.
- (18) Yesodha, S. K.; Pillai, C. K. S.; Tsutsumi, N. *Prog. Polym. Sci.* **2004**, *29*, 45–74.
- (19) Viswanathan, N. K.; Kim, D. Y.; Bian, S. P.; Williams, J.; Liu, W.; Li, L.; Samuelson, L.; Kumar, J.; Tripathy, S. K. *J. Mater. Chem.* **1999**, *9*, 1941–1955.
- (20) Hagen, R.; Bieringer, T. *Adv. Mater.* **2001**, *13*, 1805–1810.
- (21) Choi, B. Y.; Kahng, S. J.; Kim, S.; Kim, H.; Kim, H. W.; Song, Y. J.; Ihm, J.; Kuk, Y. *Phys. Rev. Lett.* **2006**, *96*, 156106.
- (22) Henzl, J.; Mehlhorn, M.; Gawronski, H.; Rieder, K. H.; Morgenstern, K. *Angew. Chem., Int. Ed.* **2006**, *45*, 603–606.
- (23) Henzl, J.; Bredow, T.; Morgenstern, K. *Chem. Phys. Lett.* **2007**, *435*, 278–282.
- (24) Alemani, M.; Peters, M. V.; Hecht, S.; Rieder, K.-H.; Moresco, F.; Grill, L. J. *Am. Chem. Soc.* **2006**, *128*, 14446–14447.
- (25) Yasuda, S.; Nakamura, T.; Matsumoto, M.; Shigekawa, H. *J. Am. Chem. Soc.* **2003**, *125*, 16430–16433.
- (26) Attianese, D.; Petrosina, M.; Vacca, P.; Concilio, S.; Iannelli, P.; Rubina, A.; Bellone, S. *IEEE Electron Device Lett.* **2008**, *29*, 44–46.
- (27) Li, N.; Lu, J.; Xu, Q.; Wang, L. *Opt. Mater.* **2006**, *28*, 1412–1416.
- (28) Bortocariu, C.; Rochon, P. *Macromolecules* **2005**, *28*, 9526–9538.
- (29) Bartkowiak, W.; Lipinski, J. *J. Phys. Chem. A* **1998**, *102*, 5236–5240.
- (30) Grasso, D.; Millefiori, S.; Fasone, S. *Spectrochim. Acta A* **1975**, *31*, 187–189.
- (31) Lee, Y. Z.; Chen, X. W.; Chen, S. A.; Wei, P. K.; Fann, W. S. *J. Am. Chem. Soc.* **2001**, *123*, 2296–2307.
- (32) Liu, Y.; Liu, M. S.; Jen, A. K.-Y. *Acta Polym.* **1999**, *50*, 105–108.
- (33) Liu, C.-Y.; Bard, A. J. *Chem. Mater.* **1998**, *10*, 840–846.
- (34) Frisch, M. J.; Trucks, G. W.; Schlegel, H. B.; Scuseria, G. E.; Robb, M. A.; Cheeseman, J. R.; Montgomery, J. A., Jr.; Vreven, T.; Kudin, K. N.; Burant, J. C.; Millam, J. M.; Iyengar, S. S.; Tomasi, J.; Barone, V.; Mennucci, B.; Cossi, M.; Scalmani, G.; Rega, N.; Petersson, G. A.; Nakatsuji, H.; Hada, M.; Ehara, M.; Toyota, K.; Fukuda, R.; Hasegawa, J.; Ishida, M.; Nakajima, T.; Honda, Y.; Kitao, O.; Nakai, H.; Klene, M.; Li, X.; Knox, J. E.; Hratchian, H. P.; Cross, J. B.; Bakken, V.; Adamo, C.; Jaramillo, J.; Gomperts, R.; Stratmann, R. E.; Yazyev, O.; Austin, A. J.; Cammi, R.; Pomelli, C.; Ochterski, J. W.; Ayala, P. Y.; Morokuma, K.; Voth, G. A.; Salvador, P.; Dannenberg, J. J.; Zakrzewski, V. G.; Dapprich, S.; Daniels, A. D.; Strain, M. C.; Farkas, O.; Malick, D. K.; Rabuck, A. D.; Raghavachari, K.; Foresman, J. B.; Ortiz, J. V.; Cui, Q.; Baboul, A. G.; Clifford, S.; Cioslowski, J.; Stefanov, B. B.; Liu, G.; Liashenko, A.; Piskorz, P.; Komaromi, I.; Martin, R. L.; Fox, D. J.; Keith, T.; Al-Laham, M. A.; Peng, C. Y.; Nanayakkara, A.; Challacombe, M.; Gill, P. M. W.; Johnson, B.; Chen, W.; Wong, M. W.; Gonzalez, C.; Pople, J. A. *Gaussian 03*, revision C.02; Gaussian Inc.: Wallingford, CT, 2004.
- (35) King, N. R.; Whale, E. A.; Davis, F. J.; Gilbert, A.; Mitchell, G. R. *J. Mater. Chem.* **1997**, *7*, 625–630.
- (36) Vijayakumar, T.; Hubert Joe, I.; Reghunadhan Nair, C. P.; Jayakumar, V. S. *Chem. Phys.* **2008**, *343*, 83–99.
- (37) Tsukamoto, T.; Liu, S.; Bao, Z. *Jpn. Appl. Phys.* **2007**, *46*, 3622–3625.
- (38) Joo, W.-J.; Choi, T.-L.; Lee, K.-H.; Chung, Y. *J. Phys. Chem. B* **2007**, *111*, 7756–7760.
- (39) Ling, Q. D.; Lim, S. L.; Song, Y.; Zhu, C. X.; Chan, D. S. H.; Kang, E. T.; Neoh, K. G. *Langmuir* **2007**, *23*, 312–319.
- (40) Weast, R. C.; Astle, M. J. *CRC Handbook of Chemistry and Physics*, 63rd ed.; CRC Press, Inc.: Boca Raton, FL, 1982–1983; p E-78.
- (41) Colle, M.; Buchel, M.; de Leeuw, D. M. *Org. Electron.* **2006**, *7*, 305–312.
- (42) Gomes, H. L.; Benvenho, A. R. V.; de Leeuw, D. M.; Colle, M.; Stallinga, P.; Verbakel, F.; Taylor, D. M. *Org. Electron.* **2008**, *9*, 119–128.

AM800001E